WAVELETS FOR BASEBAND CODING OF WAVEFORMS

*Prashant P. Gandhi, Sathyanarayan S. Rao and Ravikanth S. Pappu**

Department of Electrical and Computer Engineering
Villanova University, Villanova, PA 19085

Abstract

We consider a novel baseband waveform coding technique based on *wavelets*. Wavelets are recognized for their temporal and spectral localization and for their orthogonality across scale and location. We exploit these fundamental properties of wavelets and propose a wavelet-based modulator-demodulator structure to improve communication efficiency. Numerical results for bandwidth occupancy and bandwidth efficiency are given, and a detailed comparison between different families of wavelets is presented. A codec based on the Battle-Lemarie wavelet is shown to outperform traditional BPSK-, QPSK- and MSK-based codecs as well as codecs based on Daubechies wavelets.

1 Introduction

Wavelets have received considerable attention recently in fields such as signal processing, mathematics, physics, and seismology. This popularity of wavelets is primarily due to the interesting structure they provide based on scale (or dilation) and location (or translation). In the signal processing community itself, potential use of wavelets is currently being investigated in speech analysis and compression, image processing, video compression, radar signal processing, feature extraction and many others. In this paper, we describe a promising application of wavelets in digital communications. In particular, we propose a novel baseband coding of waveforms using wavelets.

In digital communications, a primary goal is to increase bandwidth efficiency, i.e. bit rate per unit of bandwidth (in bits/sec/Hz), without increasing the per bit signal-to-noise ratio (SNR) or the bit error rate (BER). This bandwidth efficiency is upper bounded by the Shannon limit, and the goal is to reach as close to this limit as possible. Many different modulation and coding techniques have been investigated for this purpose (see [1]). These include binary and M-ary modulation schemes, waveform shaping and channel coding. For instance, using binary phase shift keying (BPSK) with full-width rectangular pulse and null-to-null definition for bandwidth, bandwidth efficiency of 1 bit/sec/Hz is achieved. For the same SNR and BER, bandwidth efficiency is doubled to 2 bits/sec/Hz using quadrature PSK (QPSK). Additional improvement over QPSK is attained by shaping rectangular pulses, leading to bandwidth efficient minimum shift keying (MSK) modulation scheme.

In this paper, we propose a waveform coding technique based on wavelets to improve bandwidth efficiency of a communication system. A wavelet is a signal or a waveform having desirable characteristics, such as localization in time and frequency, and orthogonality across scale and translation [2],[3]. Because of these appealing properties, wavelets appear to be promising waveforms in communications. Specifically, in this paper, we use wavelets and the related scaling functions for continuous-time analog representation of data bits. We note that bit-by-bit coding using discrete shift-orthogonal wavelet sequences has been recently considered [4] while application of wavelets for secure communications has been considered in [5],[6]. Also, wavelet based binary waveform coding has been recently proposed in [7].

The paper is organized as follows. Basic concepts of wavelets and scaling functions and some of their useful properties are described in Section 2. Binary waveform coding using wavelets and scaling functions is described in Section 3 where block diagrams of transmitter and receivers are given and bit error rate and bandwidth efficiency are computed for several types of wavelets. Extension of the wavelet technique to QPSK is then proposed and compared to traditional QPSK and MSK techniques in Section 4. We end the paper with some concluding remarks in Section 5.

2 Basic Concepts of Wavelets

Briefly, let $\psi(t)$ be a (mother) wavelet. A dilated (or scaled) and translated wavelet $\psi_{j,k}(t)$ of $\psi(t)$ is given by

$$\psi_{j,k}(t) = 2^{-j/2}\psi(2^{-j}(t - 2^j k)), \tag{1}$$

where 2^j and $2^j k$ indicate the amount of dilation and translation for some integers j and k. It can be shown that the inner product between $\psi_{j,k}(t)$ and $\psi_{m,n}(t)$ for some integers j, k, m, n is

$$\langle \psi_{j,k}(t), \psi_{m,n}(t) \rangle = \int_{-\infty}^{\infty} \psi_{j,k}(t)\psi_{m,n}(t)dt = \delta_{j-m}\delta_{k-n}, \tag{2}$$

which implies that dilated and translated wavelets are orthogonal to each other.

Wavelets are unit-energy bandpass functions. There also exists corresponding unit-energy lowpass functions, called *scaling functions* $\phi_{j,k}(t)$, which are generated from a mother function $\phi(t)$. Scaling functions are orthogonal across location but *not*

*R. Pappu is now with MIT Media Lab., Cambridge, MA; his Master's thesis dealt with a portion of the work presented in Section 3.

0-7803-1820-X/94 $4.00 © 1994 IEEE

across dilation; that is, for each integer j and some integers k and n, we have

$$\langle \phi_{j,k}(t), \phi_{j,n}(t) \rangle = \delta_{k-n}. \tag{3}$$

Further, for any $j \leq m$,

$$\langle \psi_{j,k}(t), \phi_{m,n}(t) \rangle = 0 \tag{4}$$

which implies that wavelets at certain dilations and arbitrary translations are orthogonal to dilated and translated scaling functions. The above orthogonality relations of wavelets and scaling functions can be derived using the theory of multiresolution signal analysis [2]. These relations are the basis of the baseband waveform coding application presented in Section 3.

There exist many families of wavelets and scaling functions. For example, the well-known Haar wavelet (see Figures 1(a)-(b)) is given by $\psi(t) = 1/2$ for $0 \leq t < 1/2$ and $= -1/2$ for $1/2 \leq t < 1$ and has corresponding scaling function $\phi(t) = 1$ for $0 \leq t < 1$. Orthogonality properties (2)-(4) can be easily verified in this case. Note that both Haar wavelet and corresponding scaling function are commonly used to represent digital information in communication systems where Haar scaling function is generally referred to as full-width rectangular pulse and Haar wavelet as biphase pulse.

Due to the temporal discontinuity, however, the spectrum of the Haar wavelet does not decay rapidly. Wavelets that are smoother than the Haar wavelet do exist, and they offer better temporal as well as spectral localization. We consider two well-known wavelet families in this paper; they are commonly referred to as Daubechies family of wavelets and Battle-Lemarie wavelets.

Daubechies Wavelets [3] The Haar wavelet is an extreme example of Daubechies family of wavelets. A Daubechies mother wavelet D_M of order M, $M \geq 2$ and even, has following properties:

- it has finite temporal support in $[0, M-1]$,
- it is generated using an M-tap FIR filter, and
- its spectrum has a null at 2 Hz.

The wavelet D_2 is the Haar function and is the only discontinuous wavelet of this family. As the order M increases, the D_M wavelet becomes increasingly smoother and longer (see Figure 1(c)-(f)).

Battle-Lemarie Wavelet (see [2]) This wavelet is defined using cubic spline functions and is quite appealing in communications application because it has rapidly decaying spectrum (see Figure 1(g)-(h)). Although theoretically an infinite-tap filter is required to generate it, a finite-tap filter of dominant coefficients is sufficient. We show in the next section that Battle-Lemarie wavelet significantly improves bandwidth efficiency when compared to the Daubechies family of wavelets.

3 Binary Waveform Coding Using Scaling Functions and Wavelets

In the traditional BPSK modulator (see Figure 2), polar signaling is used to encode each bit prior to modulation. That is, a binary "1" is represented by a pulse $p(t)$ of duration T_b, and a binary "0" is represented by $-p(t)$. This polar signaling scheme is efficient in that, for given bit energy, it provides maximum separation between the two bit signals and thus yields the lowest probability of bit error among other binary modulation schemes (on-off, orthogonal, etc.).

Let $\{A_j\}$ be a sequence of statistically independent symbols, each assuming the value $\sqrt{E_b}$ for bit "1" or $-\sqrt{E_b}$ for bit "0", where E_b is the bit energy. A polar (baseband) signal based on pulse $p(t)$ may then be represented as

$$x_p(t) = \sum_{j=-\infty}^{\infty} A_j p(t - jT_b) \tag{5}$$

where T_b is the bit duration ($R_b = 1/T_b$ is the bit rate) and $p(t)$ is a unit-energy continuous-time pulse of duration T_b (e.g. the full-width rectangular pulse). In the presence of additive white Gaussian noise, the optimum receiver is a matched filter with impulse response function $p(T_b - t)$, followed by sampler and a hard-limiter. For passband binary phase shift keying (BPSK), baseband signal (5) is used to modulate the carrier $\cos(\omega_c t)$, where ω_c is the carrier frequency.

With $p(t)$ being the full-width rectangular pulse, we may say that information bits in (5) are coded using the D_2 (or Haar) scaling function. This D_2 scaling function however does not have appealing spectral characteristics; so it is natural to consider other scaling functions that do have desirable characteristics. Replacing $p(t)$ in (5) with a suitable scaling function $\phi(t)$, we get

$$x_\phi(t) = \sum_{j=-\infty}^{\infty} \frac{A_j}{\sqrt{T_b}} \phi\left(\frac{t - jT_b}{T_b}\right). \tag{6}$$

Note that each scaling function in (6) is dilated by T_b. For orthogonality property (3) to hold, clearly T_b must be a power of 2 (i.e. $T_b = 2^j$ for some j). Further, mother scaling functions (except D_2) that we consider here have temporal support larger than unity. Thus each dilated scaling function in (6) has temporal duration $T > T_b$. A D_M scaling function, for example, is of duration $T = (M-1)T_b$. Block diagrams of scaling function-based baseband modulator and demodulator are given in Figure 3. Figure 4 shows a typical polar signal representing bit sequence $\cdots\ 1\ 0\ 0\ 1\ \cdots$. The same bit sequence, coded using D_4 scaling functions, is shown in Figure 5(a).

Since information bits arrive at rate $R_b = 1/T_b$, it is easy to see that scaling functions corresponding to neighboring bits *overlap*. This is evident from Figure 5(a). The resulting polar signal is depicted in Figure 5(b). Decoding of bits is possible because, according to (3), any pair of scaling functions separated by integer multiple of T_b are orthogonal. Specifically, at the receiver (see Figure 3), impulse response of the matched filter is given by $\phi(\frac{JT_b - t}{T_b})/\sqrt{T_b}$ where $T = JT_b$ is the duration of $\phi(t/T_b)$ for some integer $J > 1$. Assuming noiseless transmission medium, the matched filter output $y(t)$, sampled at $t = nT_b$, is

$$\begin{aligned} y(t = nT_b) &= x_\phi(t) * T_b^{-1/2} \phi\left(\frac{JT_b - t}{T_b}\right)\Big|_{t=nT_b} \\ &= \sum_{j=-\infty}^{\infty} \frac{A_j}{T_b} \int_{(n-J)T_b}^{nT_b} \phi\left(\frac{\tau - jT_b}{T_b}\right) \phi\left(\frac{\tau - (n-J)T_b}{T_b}\right) d\tau \\ &= A_{n-J} \end{aligned} \tag{7}$$

Clearly, from (7), information bits are recovered at the receiver at rate R_b after an initial delay of JT_b (see Figure 5(c) where $J = M - 1 = 3$).

Bit error probability (BER), in the presence of additive white Gaussian noise, can also be computed easily. For shift-orthogonal waveforms $\phi(t/T_b)$, the receive BER can be calculated from the BPSK (or polar) signal space diagram. It is therefore not surprising to see that, for equal bit energies, the BER for (6) is *identical* to the one for (5). Hence, comparison between the two methods should only be based on their bandwidth utilizations.

Before proceeding to the determination of bandwidth efficiencies, we list some key features of scaling function-based waveform coding technique:

- neighboring waveforms overlap;
- decoder outputs are delayed by JT_b;
- output bit rate is identical to the input rate;
- T_b must be a power of 2; and
- BER is equal to the BER of BPSK scheme.

The above scheme can be generalized to include both scaling functions and wavelets as shown in Figure 6. Here the composite baseband signal is a sum of two polar signals – one coded using scaling functions and the other using wavelets:

$$x_{\phi\psi}(t) = \sum_{j=-\infty}^{\infty} \frac{A_j}{\sqrt{T_b}}\phi(\frac{t-jT_b}{T_b}) + \sum_{j=-\infty}^{\infty} \frac{B_j}{\sqrt{T_b}}\psi(\frac{t-jT_b}{T_b}). \quad (8)$$

Here zero-mean random variables $\{A_j\}$ and $\{B_j\}$ are assumed to be individually and jointly independent. A corresponding passband signal is obtained by modulating a single carrier $\cos(\omega_c t)$ using (8). Decoding is possible, as shown in Figure 6, due to the self- and cross-orthogonality properties of $\phi(t/\sqrt{T_b})$ and $\psi(t/\sqrt{T_b})$ functions. The bit error rate again remains equal to the BPSK scheme as we are dealing with two independent polar signals. Further, the data rate is doubled and so is the overall bandwidth, as seen in Figure 7(a).

To compare different wavelet-based coding techniques, we employ the bandwidth efficiency (BE) measure defined by

$$BE = \frac{\text{Total Bit Rate}}{\text{Bandwidth}} \quad \text{(bits/sec/Hz)} \quad (9)$$

where we assume 99% power bandwidth. Power spectral densities (psd) of the composite scheme (8) for several Daubechies waveforms as well as Battle-Lemarie waveforms are shown in Figure 7(b). Clearly, psd of composite coding scheme based on Battle-Lemarie waveforms has better decay characteristics than those based on Daubechies waveforms. Numerical comparisons are given in the table given below. Here the 99% bandwidth (BW) is normalized with respect to the bit period T_b. As seen from the table, BE improves with higher orders of Daubechies waveforms; Battle-Lemarie waveforms give the best performance.

Wavelet	*BW*	*BE*
D_2 (Haar)	3.5	0.57
D_4	3.1	0.65
D_6	2.8	0.71
D_8	1.4	1.43
D_{10}	1.35	1.48
Battle-Lemarie	1.15	1.74

Table 1: Comparison of different coding techniques

4 Wavelet Based QPSK Codec

With the inclusion of scaling functions and wavelets, we have shown in the above section that two independent bit sequences $\{A_j\}$ and $\{B_j\}$ can be multiplexed, resulting in an improved BE value. Improvement is primarily due to the fact that bandwidth conserving waveforms are used for baseband waveform coding. It is well-known that, for passband modulation, orthogonal *carrier* waveforms $\sin(\omega_c t)$ and $\cos(\omega_c t)$ may be used to obtain further improvement in BE without affecting the bit error probability.

Let $\{A_j^I\}$ be the in-phase and $\{A_j^Q\}$ be the quadrature sequence of statistically independent symbols $\pm\sqrt{E_b}$, as before. With $p(t)$ the analog pulse representing symbol A_j^I or A_j^Q, a QPSK signal may be written as

$$x_p^Q(t) = \sum_{j=-\infty}^{\infty} A_j^I p(t-jT_b)cos(\omega_c t) + A_j^Q p(t-jT_b)sin(\omega_c t). \quad (10)$$

With the in-phase and quadrature symbol sequences being mutually independent, it is easy to see that (10) is composed of two independent BPSK signals. Therefore, the BER using (10) is identical to that using a BPSK signal based on (5). However, essentially two bits are transmitted in a given bit period, and thus a doubling of BE is achieved. To improve BE further, the maximum phase discontinuity of $\pm\pi$ in QPSK is reduced to $\pm\pi/2$ in MSK by shifting the in-phase signal by $T_b/2$ units [1]. Further, low-frequency sinusoids are used instead of rectangular pulses, thus yielding a spectrally efficient MSK signal.

A QPSK-type codec using scaling functions and wavelets can also be designed using the ideas of Section 3. Based on the results obtained in Section 3 for BPSK signaling, it is intuitively clear that a QPSK extension of the wavelet codec can give significant improvement in BE. Let $x_\phi^Q(t)$ be the scaling function-based QPSK signal defined by (10) with $p(t)$ replaced by $\phi(t/T_b)/\sqrt{T_b}$; let wavelet-based $x_\psi^Q(t)$ be similarly defined using independent symbol sequences $\{B_j^I\}$ and $\{B_j^Q\}$ and waveform $\psi(t/T_b)/\sqrt{T_b}$. A wavelet-based QPSK (WQPSK) signal $x_{\phi\psi}^{WQ}(t)$ is then given by (see Figure 8)

$$\begin{aligned} x_{\phi\psi}^{WQ}(t) &= x_\phi^Q(t) + x_\psi^Q(t) \\ &= \sum_{j=-\infty}^{\infty} \left[\frac{A_j^I}{\sqrt{T_b}}\phi(\frac{t-jT_b}{T_b}) + \frac{B_j^I}{\sqrt{T_b}}\psi(\frac{t-jT_b}{T_b})\right] cos(\omega_c t) + \\ &\quad \left[\frac{A_j^Q}{\sqrt{T_b}}\phi(\frac{t-jT_b}{T_b}) + \frac{B_j^Q}{\sqrt{T_b}}\psi(\frac{t-jT_b}{T_b})\right] sin(\omega_c t) \end{aligned} \quad (11)$$

Thus, using orthogonal waveforms at baseband *and* at radio frequency, a total of four rate-R_b sequences $\{A_j^I\}$, $\{A_j^Q\}$, $\{B_j^I\}$ and $\{B_j^Q\}$ are multiplexed to yield a single WQPSK signal $x_{\phi\psi}^{WQ}(t)$. Clearly, this WQPSK signal carries *four* bits of information per bit duration T_b whereas QPSK and MSK signals carry only two bits of information per T_b. A judicious selection of $\phi(t)$ and $\psi(t)$ can yield a spectrally appealing composite signal.

As in the case of BPSK, the average bit error rate of WQPSK is the same as QPSK. Thus a comparison of BE among different QPSK signaling schemes is sufficient. Figure 9 depicts out-of-band power (in dB) as a function of normalized bandwidth for

BPSK, QPSK, MSK and WQPSK (using Battle-Lemarie waveforms). It is clear from the figure that 99%-power (i.e. -20 dB out-of-band power) bandwidth for MSK is much lower than that for WQPSK. If we increase the in-band power requirement to 99.9%, both signals require the same (normalized) bandwidth of about 1.25 Hz. Since WQPSK signal carries more information per bit period than MSK signal (4 bits versus 2 bits), its BE is significantly better. This is shown in Table 2.

Signal	*99% BW*	*BE*	*99.9% BW*	*BE*
QPSK	~2.50	0.80	–	–
MSK	0.55	3.63	1.25	1.6
WQPSK	1.15	3.48	1.25	3.2

Table 2: Comparison of different QPSK coding techniques

5 Concluding Remarks

We have proposed an interesting method for coding of waveforms using wavelets and scaling functions. Its operation is possible due to the scale and location orthogonality of wavelets and scaling functions. Wavelet-based codecs for BPSK and QPSK modulation schemes are described and shown to give improved spectral characteristics.

References

[1] B. Sklar, *Digital Communications*, Prentice Hall, 1988.

[2] S. Mallat, "A theory of multiresolution signal decomposition: the wavelet representation," *IEEE Trans. on Pattern Analysis and Machine Intelligence*, pp. 674-693, July 1989.

[3] I. Daubechies, "The wavelet transform, time-frequency localization and signal analysis," *IEEE Trans. on Information Theory*, pp. 961-1005, September 1990.

[4] M. Tzannes and M. Tzannes, "Bit-by-bit channel coding using wavelets," In *Proc. of GLOBECOM*, 1992.

[5] D. Cochran and C. Wei, "Scale Based Coding of Digital Communication Signals," In *Proc. of IEEE-SP Intl. Symp. Time-Freq and Time-Scale*, pp. 455-458, October 1992.

[6] R. Orr, et. al, "Covert Communications Employing Wavelet Technology," In *Proc. of 27th Asilomar Conference on Signals, Systems and Computers*, November 1993.

[7] P. P. Gandhi,S. S. Rao and R. S. Pappu, "On Waveform Coding Using Wavelets," *Proc. of 27th Asilomar Conference on Signals, Systems and Computers*, November 1993.

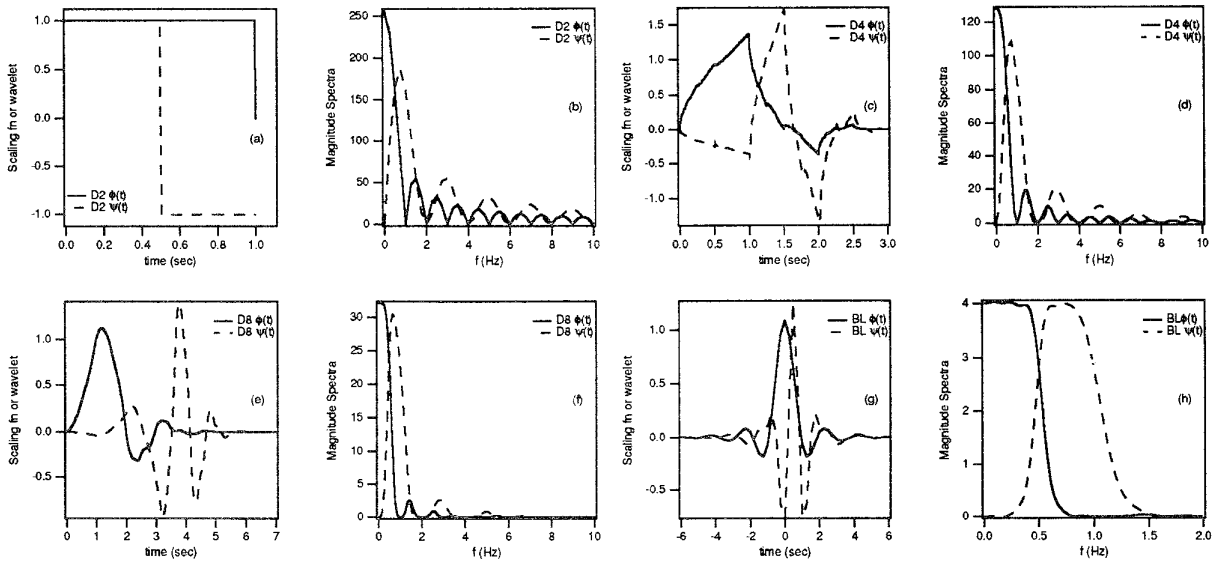

Figure 1: Scaling Functions, wavelets and their magnitude spectra

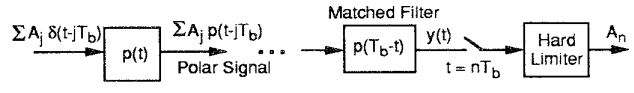

Figure 2: Block diagrams of baseband polar transmitter and receiver

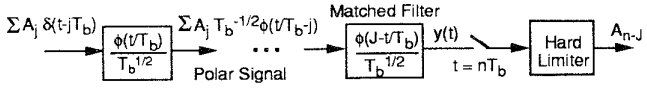

Figure 3: Block diagrams of transmitter and receiver based on scaling function

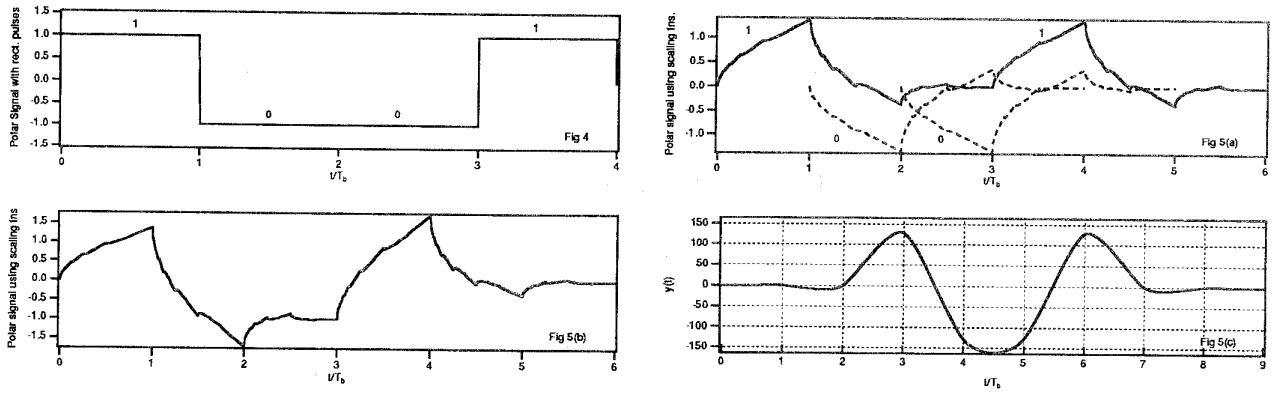

Figures 4: Polar signal using rectangular pulses; Figure 5: (a) D4 scaling functions corresponding to information bits 1001, (b) polar signal using D4 scaling function, (c) matched filter output.

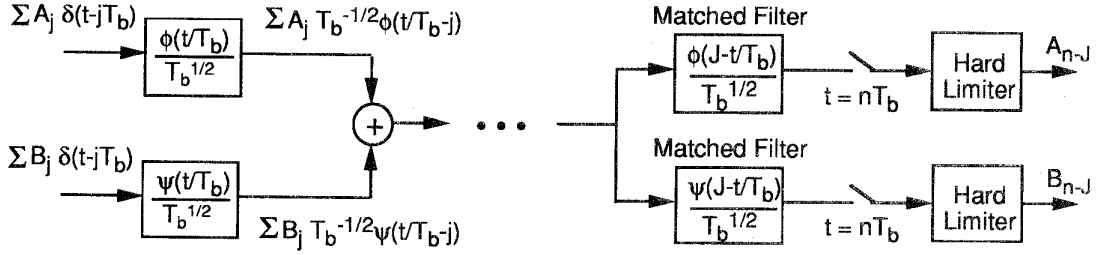

Figure 6: Block diagrams of transmitter and receiver based on scaling function and wavelet

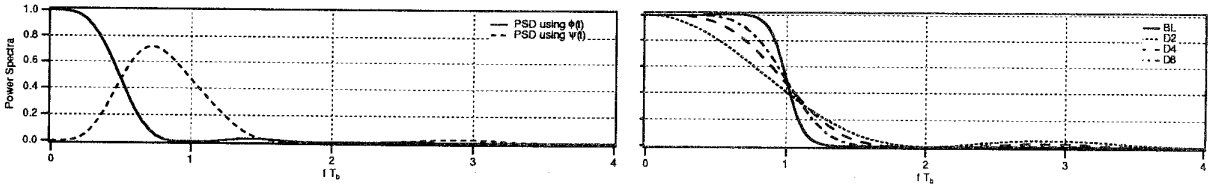

Figure 7: (a) PSD of polar signal using D4 scaling function or wavelet, (b) Normalized PSD of composite signal

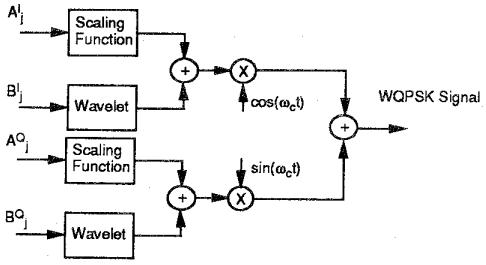

Figure 8. WQPSK transmitter

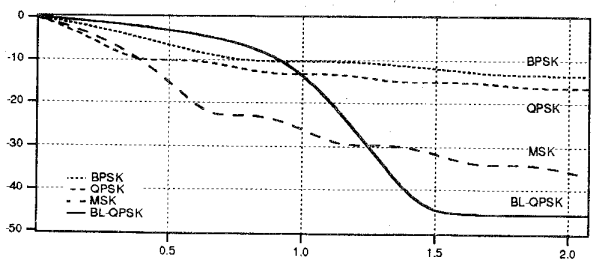

Figure 9: Out-of-band power comparisons

Coordinate Interleaving TCM for Flat Fading and AWGN Channels

B. Jeličić & S. Roy*
Dept. of Electrical Engineering
University of Pennsylvania
Philadelphia, PA 19104

Abstract

In [3] a new algorithmic approach for designing QAM-TCM schemes based on coordinate interleaving [2] was introduced. Simulations performed under ideal assumptions showed significant coding gains with respect to standard TCM schemes. In this work, we undertake a more thorough investigation of code performance including the effects of finite interleaving and imperfect channel state information (CSI). We show that despite being more sensitive to the above impairments, coordinate interleaving TCM largely preserve their coding gains and have a much lower error floor than standard symbol interleaving TCM. Finally, the coding gains observed in simulations are substantiated by cut-off rate computations.

1 Introduction

Trellis-Coded Modulation (TCM), since it's introduction a decade ago [11], has resulted in a number of useful coding schemes for bandwidth-efficient signalling over the additive white Gaussian noise (AWGN) channel. In contrast, the problem of design of good coded modulation schemes for fading channels appears to be unresolved, despite the important contributions of [1, 4, 5]. Given the emerging interest in QAM modulation for speech and data transmission for mobile systems [7, 8, 10], in this work we concentrate on QAM-TCM schemes that are effective against both non-fading (i.e., AWGN) and flat fading conditions. Incorporating the principle of *interleaving over coordinates* from [2], we present a a new algorithm for signal set design that achieves good diversity over fading channels while preserving coding gain over AWGN channels. Some preliminary work under ideal model assumptions in [3] showed large coding gains with respect to standard TCM schemes. Here, we investigate the effects of several practical issues on code implementation and performance such as finite interleaving and imperfect CSI. We show that although being more sensitive to above mentioned impairments, these new schemes largely preserve their coding gains, and more importantly, have lower error floors when compared with standard ones. Finally, cut-off rates were computed to support the observed gains.

*Author for all correspondence; FAX:(215) 573-2068; Ph: (215) 898-2260

2 TCM Over Fading & AWGN Channel

We assume a flat-fading channel that varies slowly enough so that coherent demodulation is possible. In the k-th signaling interval, the transmitter sends a two dimensional (2-D) symbol $\underline{x}_k = (x_{2k-1}, x_{2k})$, where x_{2k-1}, and x_{2k} denote corresponding in-phase (I), and quadrature (Q) components, from a QAM signal constellation of average symbol energy E_s. For the remainder of the paper, it is assumed that the signal points $\underline{x}_k$ are drawn from a 2-D constellation. If we assume a message length of N signalling intervals, it can be represented as an N-sequence of 2-D symbols $\mathbf{x} = (\underline{x}_1, \underline{x}_2, \ldots, \underline{x}_N)$, or equivalently as $\mathbf{x} = (x_1, x_2, \ldots, x_{2N})$, where $\{x_i\}_{i=1}^{2N}$ will be referred to as coordinates of the $2N$-D vector that represents a message. Assuming standard interleaving over symbols, the received sequence $\mathbf{y} = (\underline{y}_1, \underline{y}_2, \ldots, \underline{y}_N)$, is related to the transmitted symbols $\underline{x}_k$ via

$$\underline{y}_k = \rho_k \, \underline{x}_k + \underline{n}_k \tag{1}$$

where ρ_k is an i.i.d. sequence of scalar random variables representing the amplitude of the fading received signal, implying that both in-phase (I) and quadrature (Q) components fade simultaneously.

We invoke the usual assumptions that $\underline{n}_k$ is a sample of a 2-D AWGN process with independent components having power spectral density (psd) $N_0/2$, and ρ_k is a normalized ($E(\rho_k^2) = 1$) Rayleigh fading random amplitude.

Assuming perfect CSI (i.e., ρ_k are known at the receiver) and uncorrelated fading (corresponding to perfect interleaving), the appropriate decoding metric is

$$m(\mathbf{y}, \mathbf{x}; \rho) = \sum_{k=1}^{N} || \, \underline{y}_k - \rho_k \, \underline{x}_k \, ||^2 , \tag{2}$$

0-7803-1820-X/94 $4.00 © 1994 IEEE